Journal of Alloys and Compounds 509 (2011) 3246–3251

Contents lists available at ScienceDirect

Journal of Alloys and Compounds

journal homepage: www.elsevier.com/locate/jallcom

304L stainless steel oxidation in carbon dioxide: An XPS study

Fabrice Goutier, Stéphane Valette, Etienne Laborde, Pierre Lefort*

SPCTS, CNRS UMR 6638, European Ceramic Center, 12, rue Atlantis, 87068 Limoges Cedex, France

ARTICLE INFO

Article history:
Received 29 September 2010
Accepted 14 December 2010
Available online 22 December 2010

Keywords:
Metals and alloys
Gas–solid reactions
Oxidation
X-ray photoelectron spectroscopy (XPS)
CO_2

ABSTRACT

From the early beginning of the oxidation of 304L stainless steel in carbon dioxide at 1273 K (1 min, for a weight gain of 0.02 mg cm^{-2}), the surface of the alloy was entirely covered by oxides: magnetite Fe_3O_4, chromia Cr_2O_3 and traces of wüstite $Fe_{1-x}O$. Later on, for weight gains approaching 1 mg cm^{-2}, magnetite remained at the outer interface, with traces of hematite (Fe_2O_3), above a thick layer of wüstite $Fe_{1-x}O$. Magnetite and wüstite may favour adhesion of thermal plasma protective coatings such as alumina.

1. Introduction

The oxidation of 304L stainless steel in carbon dioxide has been recently studied in order to clarify the mechanism of the beginning of the reaction [1]. This work was related to a new process for plasma coating of ceramics on metals or alloys, which begins by a pre-oxidation of the alloys, for obtaining a bonding layer at their surfaces. For instance, the oxides obtained at the surface of C40E steel by oxidation in CO_2 [2] provide excellent adherences to alumina coatings *via* crystallographic relationships at the interfaces steel/wüstite/magnetite/alumina [3]. The interest of working under CO_2 is to favour the formation of wüstite $Fe_{1-x}O$ that plays the major part in such a "crystallographic bonding".

For 304L stainless steel, between 1193 and 1273 K in CO_2 (from 2×10^4 to 10^5 Pa), the reaction kinetics exhibit three successive stages:

(i) a short initial period of acceleration;
(ii) a slowing down ($0.35 < \Delta m/S < 1.15$ mg cm^{-2});
(iii) a breakaway.

The only second stage has been exhaustively analyzed kinetically because the first stage was too short and the third one had a mediocre reproducibility. However, the first stage ($\Delta m/S < 0.35$ mg cm^{-2}) is the most interesting for coating applications, as far as it corresponds to thin oxide layers on the surface. Indeed, a rather weak thickness of the interlayers favours a strong bonding of further ceramic plasma deposits [4]. In fact, there are only very few studies devoted to the early beginning of chromium steels oxidation, especially in CO_2, and the nature of the initial oxides (chromium rich iron sesquioxide, chromite or iron oxides) has been debated [5].

For these reasons, it seemed important to identify precisely the thin oxide layers formed when oxidation begins, and so, the aim of the present study was to analyze by XPS the first oxides appearing on 304L stainless steel in carbon dioxide.

2. Materials and methods

2.1. Steel and gas

Composition of 304L alloy used, from Chaumeil S.A. (Brive, France), is given in Table 1. Carbon dioxide was provided by Air Liquide France; this gas of mediocre quality was chosen in order to reproduce industrial conditions: at 10^5 Pa and 288 K, purity 99.7 vol.%, with 200 volume ppm H_2O.

2.2. Oxidation of 304L steel

Oxidations were carried out in a thermobalance (Setaram B70) equipped with a $MoSi_2$ furnace where carbon dioxide was introduced at 10^5 Pa (static atmosphere). Samples of 304L were small disks (10 mm diameter, 1 mm thick, with a hole of 1 mm diameter for holding them), polished up to SiC papers grit 4000. Once the convenient temperature reached (1273 K), samples were moved into the hot zone for different times. Before cooling, oxidized samples were quenched in the cold part of the furnace [1].

2.3. Sample characterization

Surface analyzes by XPS were realized with a Kratos Axis Ultra spectrometer using a monochromatic source Al Kα (1486.6 eV) obtained with an accelerating voltage of 15 kV and a current intensity of 12 mA. The area analyzed was

* Corresponding author at: University of Limoges, European Ceramic Center, 12, rue Atlantis, 87068, Limoges Cedex, France.
Tel.: +33 0 587 50 23 42; fax: +33 0 587 50 23 04.
E-mail address: pierre.lefort@unilim.fr (P. Lefort).

0925-8388/$ – see front matter © 2010 Elsevier B.V. All rights reserved.
doi:10.1016/j.jallcom.2010.12.094

Table 1
Composition of the 304L stainless steel.

	Element										
	C	Si	Mn	P	S	Cr	Ni	Co	Cu	N	Fe
wt.%	0.024	0.240	1.340	0.033	0.026	18.060	8.100	0.200	0.360	0.0830	71.534

300 μm × 700 μm. The pass energy was 20 eV for the high-resolution spectra and 160 eV for the surveys. The spectrometer was calibrated with standard elements gold and copper. A compensation of charges (*in situ* correction) was applied and the positions were corrected in reference to the 1 s spectroscopic state of carbon (285 eV), in order to eliminate any perturbation (charge effects, surface state, etc.).

The X-ray patterns presented in the discussion part were obtained with a SIEMENS D5000 X-ray diffractometer (radiation Cu Kα) equipped with a back monochromator. The scanned angles (in 2θ scale) ranged between 20° and 80° with a step of 0.02° and a 0.9 s exposure time. The X-ray patterns were indexed with DIFFRAC+ software (Socabim) containing JCPDS files database.

3. Results

3.1. Global survey

The surfaces of five samples with different oxidation degrees were analyzed by XPS. Their global surveys by XPS are presented in Fig. 1. One sample was not oxidized (Fig. 1a), the others were treated at 1273 K in 10^5 Pa of carbon dioxide during 5 min ($\Delta m/S \approx 0.09$ mg cm^{-2}, Fig. 1b), 15 min ($\Delta m/S \approx 0.3$ mg cm^{-2}, Fig. 1c) and 1 h ($\Delta m/S \approx 1$ mg cm^{-2}, Fig. 1d).

For all of them, the following peaks appeared:

(i) iron (2p signal from 705 to 730 eV);
(ii) manganese (2p signal from 638 to 665 eV);
(iii) oxygen (1 s signal from 528 to 535 eV);
(iv) chromium (2p signal from 572 to 594 eV), peak missing for the sample oxidized 1 h;
(v) carbon (1 s signal from 282 to 290 eV).

The intensity of manganese and chromium signals increases during the first 5 min of oxidation (up to $\Delta m/S \approx 0.09$ mg cm^{-2}) and then decreases. After 1 h ($\Delta m/S \approx 1$ mg cm^{-2}), there are only traces of manganese at the surface and chromium completely vanished. Nickel, well detected by its signal 2p in the non-oxidized steel, is missing on the oxidized surfaces.

3.2. High resolution spectrum

3.2.1. Chromium spectrum

The deconvolution of the $2p_{3/2}$ chromium signal of a sample oxidized 1 min (weight gain of 0.02 mg cm^{-2}) required five peaks as seen in the Fig. 2 that shows a good fit between the sum of the five peaks (bold line) and the original spectrum (fine line). The Shirley-type background is drawn as baseline. As long as the chromium was detected, its spectrum had the same shape, whatever the weight gain could be. Fig. 2 provides also the exact position and the full width at half maximum (FWHM, in eV) of each peak.

3.2.2. Iron spectrum

Fig. 3 presents the $2p_{3/2}$ spectrum of iron for a weight gain of 0.02 mg cm^{-2} with its deconvolution, the baseline (Shirley-type background), and the characteristics of each peak. No shoulder was seen on the right part of the spectrum, *i.e.* for the low-binding energies, as sometime seen in such cases [6]. Deconvolution revealed 4 peaks related to the ions Fe^{2+} and 5 peaks for Fe^{3+}. The components of the high spin (3d electron not coupled) Fe^{2+} can be described by

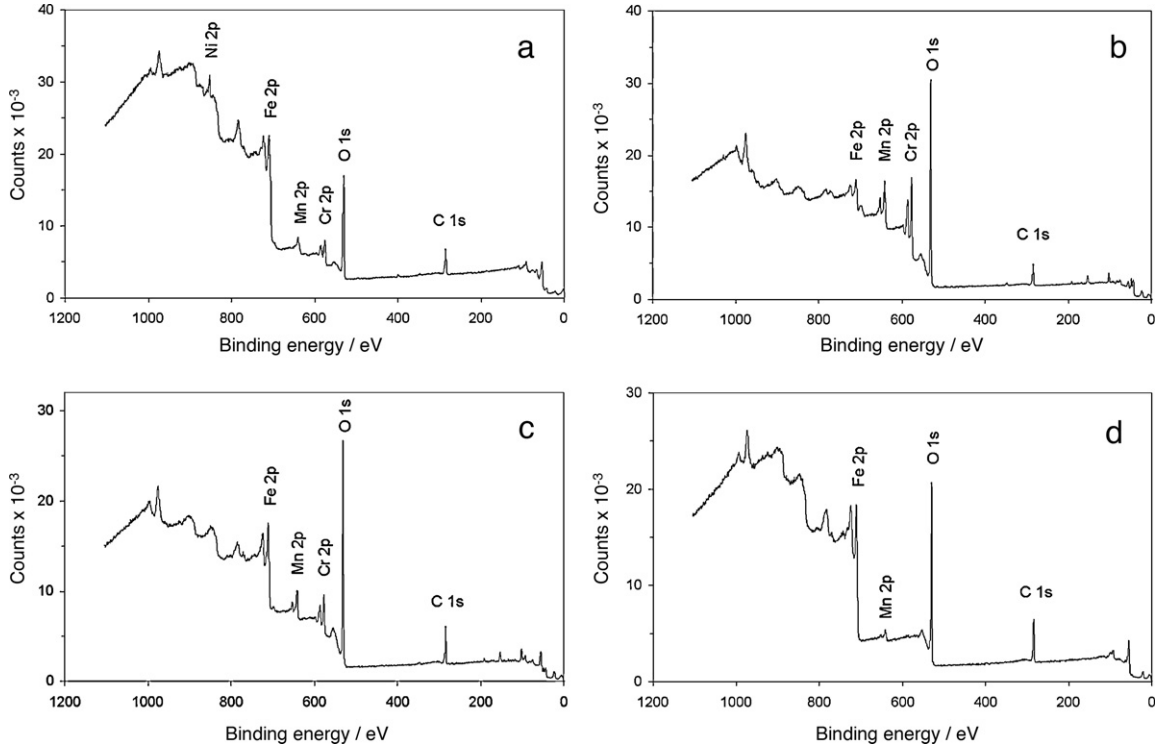

Fig. 1. XPS global survey of the surfaces of samples non-oxidized (a) and oxidized at a weight gain of 0.09 mg cm^{-2} (b), 0.3 mg cm^{-2} (c) and 1 mg cm^{-2} (d).

	Position (eV)	FWHM (eV)
Peak 1	576.2	1.1
Peak 2	577.1	1.1
Peak 3	577.8	0.9
Peak 4	578.6	0.9
Peak 5	579.4	1.0

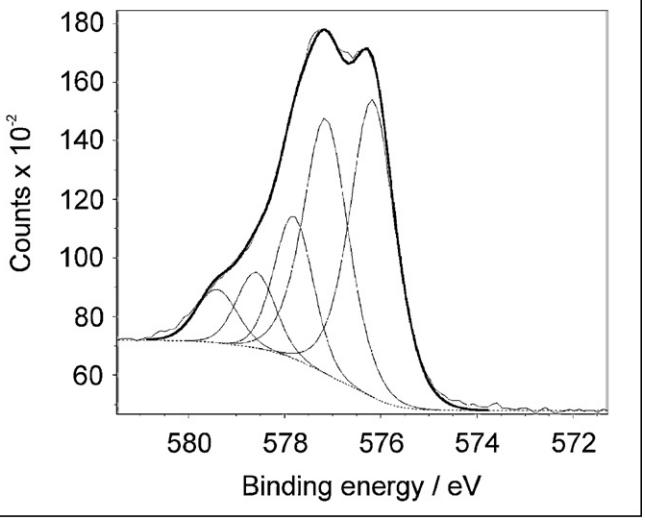

Fig. 2. XPS profile of the $2p_{3/2}$ spectroscopic state of chromium at the surface of the oxidized steel ($\Delta m/S \approx 0.02\,mg\,cm^{-2}$).

a triplet and one satellite peak, as previously reported [7,8]. The high spin Fe^{3+} is described by a quadruplet and one satellite peak, in good agreement with Grosvenor et al. works [7]. The satellite peaks, whose FWHM is larger than that of the components of the multiplets, are usually considered as due to the shift of electrons 3d to the 4 s vacant level during ejection of a photoelectron of core [9]. Thus, the Fe^{2+} and Fe^{3+} states could be clearly identified, and the same kind of spectrum was found all the reaction long.

The characteristics (position, FWHM in square brackets and proportion in bold type) of all the deconvolution peaks, for the multiplets of the Fe^{2+} and Fe^{3+} cations, are reported in Table 2. The values obtained on stoichiometric wüstite and magnetite with the same spectrometer by Grosvenor et al. [7] are in italics.

Experimental profiles are very well reconstructed with these multiplets (e.g. in Fig. 3, the fine experimental line to be compared with the bold line corresponding to the reconstructed spectrum). The chemical environment of the cations is sensibly the same for the oxidation durations considered, as indicated by the constant position of the deconvolution peaks (Table 2).

4. Discussion

An important point to be noticed first is that, even at the early beginning ($\Delta m/S \approx 0.02\,mg\,cm^{-2}$), the surface of the alloy was entirely covered by an oxide layer. This was established because the element nickel, one of the major components of the alloy, was no

	Position (eV)	FWHM (eV)	%
Peak 1 (Fe^{2+})	708.6	1.3	34
Peak 2 (Fe^{2+})	709.6	1.2	36.5
Peak 3 (Fe^{2+})	710.9	1.4	29.5
Peak 4 (Fe^{3+})	710.2	1.4	33.2
Peak 5 (Fe^{3+})	711.5	1.4	32.4
Peak 6 (Fe^{3+})	712.6	1.4	25.3
Peak 7 (Fe^{3+})	713.9	1.4	9.1
Peak 8 (Fe^{2+})	714.5	4.1	-
Peak 9 (Fe^{3+})	716.8	2.3	-

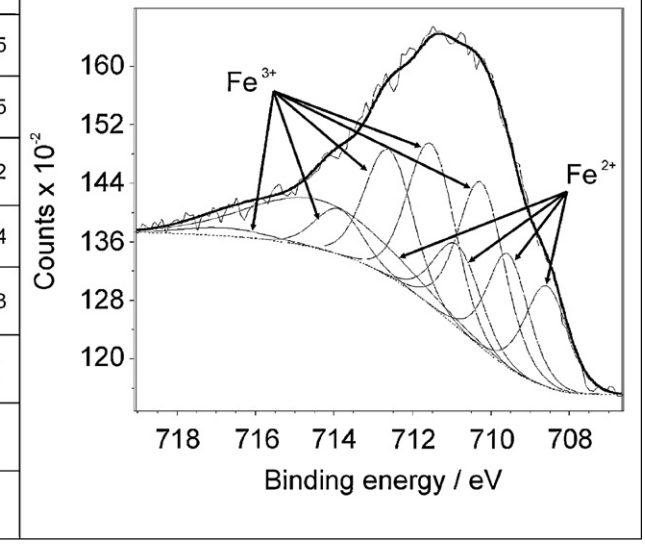

Fig. 3. XPS profile of the $2p_{3/2}$ spectroscopic state of iron at the surface of the oxidized steel ($\Delta m/S \approx 0.02\,mg\,cm^{-2}$)

Table 2
Position of the deconvolution peaks obtained with theoretical considerations (first value, in eV), width at half maximum (between brackets, in eV) and proportion within the multiplet (in bold type, %).

		Fe^{2+} multiplet			Fe^{3+} multiplet				Satellites peaks		
		Peak 1	Peak 2	Peak 3	Peak 4	Peak 5	Peak 6	Peak 7	Peak 8	Peak 9	Peak 10
Weight gain / mg cm^{-2}	0.02	708.6 [1.3] **34.0**	709.6 [1.2] **36.5**	710.9 [1.4] **29.5**	710.2 [1.4] **33.2**	711.5 [1.4] **32.4**	712.6 [1.4] **25.3**	713.9 [1.4] **9.1**	714.5 [4.1]	716.8 [2.3]	-
	1	708.6 [1.2] **31.4**	709.6 [1.2] **39.6**	710.8 [1.4] **29.0**	710.4 [1.4] **30.4**	711.5 [1.4] **31.1**	712.6 [1.4] **24.3**	713.7 [1.4] **14.2**	715.0 [2.0]	716.6 [1.5]	718.5 [1.9]
Fe_3O_4 [7]		*708.3 [1.2]* ***41.6***	*709.3 [1.2]* ***43.2***	*710.4 [1.4]* ***15.2***	*710.2 [1.4]* ***34.9***	*711.3 [1.4]* ***31.8***	*712.4 [1.4]* ***22.6***	*713.6 [1.4]* ***10.8***			
FeO [7]		*708.4 [1.4]* ***35.2***	*709.7 [1.6]* ***43.7***	*710.9 [1.6]* ***21.1***							

Key → Position (eV) / [FWHM, in eV) / **Proportion (%)**

longer visible after only 60 s of treatment, when the thermal equilibrium of the sample was hardly reached. This result is somewhat surprising, since metals oxidation generally begins by the formation of germs growing progressively [10]. Here, germination and growth of the oxides were obviously very rapid, covering the entire surface in less than 1 min, when they were missing on non-oxidized samples.

4.1. Nature of the surface phases

Now, it is interesting is to identify the phases present at the surface of the samples, and to follow their changes with time. For this, XRD analyzes were carried out in order to compare them with the XPS results. Such as for XPS analyzes, X-ray patterns were obtained on samples non-oxidized, and oxidized at $\Delta m/S \approx 0.09\,mg\,cm^{-2}$, $0.3\,mg\,cm^{-2}$ and $1\,mg\,cm^{-2}$ (for $\Delta m/S \approx 0.02\,mg\,cm^{-2}$ nothing was visible except the substrate). These patterns, presented in Fig. 4, show that chromia is seen only at the beginning ($\Delta m/S \approx 0.09\,mg\,cm^{-2}$), the major oxides being a spinel phase ($\Delta m/S \approx 0.3\,mg\,cm^{-2}$) and wüstite ($\Delta m/S \approx 1\,mg\,cm^{-2}$). On the basis of the position of the peaks, the spinel phase could be magnetite, but it is assumed that it was a chromite phase, type $FeCr_2O_4$, with variable composition in view of the large width of its peaks. Indeed, chromium being the most oxidizable component of the alloy, and as far as chromia vanished rapidly, the spinel phase necessarily contains this element.

The peaks of the substrate are visible on all the patterns, which means that XRD analyzes concern the entire layer of oxides, from

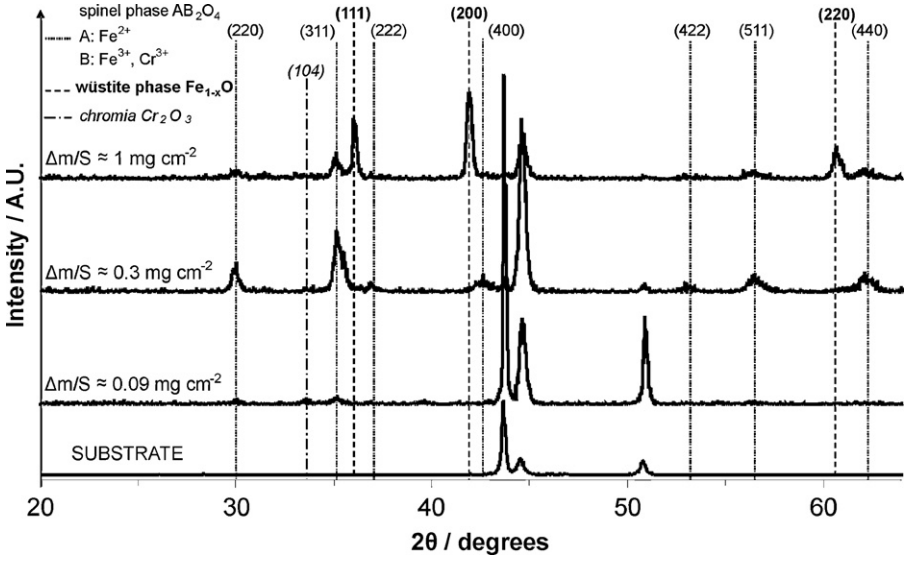

Fig. 4. XRD patterns of the surface of samples non-oxidized and oxidized at different weight gains.

the outer surface to the alloy, corresponding to a thickness of 2 μm at least ($\Delta m/S \approx 0.09\,mg\,cm^{-2}$), which is a major difference compared to XPS that analyzes only the first atomic layers.

However, it clearly appears that great changes affect the oxides layer during the first hour of oxidation. So, at the early beginning ($\Delta m/S \leq 0.09\,mg\,cm^{-2}$):

(i) Chromium (accompanied by manganese as generally observed in oxidation of iron-based alloys [11]) appears in great quantities. In its spectrum XPS, the presence of the peak at 579.4 eV (Fig. 2) means that chromium is present in an environment Cr_2O_3 or spinel such as $NiCr_2O_4$ [12]. As far as nickel is missing in the oxide layer, it is clear that chromium belongs to a chromia phase Cr_2O_3, in good agreement with XRD results.
(ii) XPS shows that iron oxidizes simultaneously in a phase containing both Fe^{2+} and Fe^{3+}. In the studied system, three phases are possible:
- wüstite $Fe_{1-x}O$, mainly composed of Fe^{2+} with Fe^{3+} in quantity depending on the value of x;
- magnetite Fe_3O_4 that contains 1 Fe^{2+} for 2 Fe^{3+};
- chromite $FeCr_2O_4$.

The comparison with the previous results of Grosvenor et al. [7] provided in Table 2 shows that the position and the proportions of the peaks observed here are close to those given for the magnetite Fe_3O_4. Consequently, the formation of chromite appears as unlikely, because the presence of ions Cr^{3+} in the spinel structure would probably shift the position of the peaks, but no data is available on this point.

About wüstite XRD did not detect its presence quantitatively before $\Delta m/S \approx 0.35\,mg\,cm^{-2}$. Otherwise, it can be observed that Grosvenor et al. [7] did not provide the spectrum of wüstite but that of $Fe_{1.1}O$, that is to say a mix of pure iron and of monoxide FeO, obtained by reduction of hematite Fe_2O_3. This explains why these authors gave no peak of Fe^{3+} for this phase: contrary to wüstite, $Fe_{1.1}O$ contains only Fe^{2+}. But, the data of Table 2 show that the positions and the proportions of ions Fe^{2+} found here are closer to those of iron monoxide than to those of magnetite, and the ratio of the Fe^{3+}/Fe^{2+} peaks areas is of 1.8, *i.e.* between $Fe_{1-x}O$ and Fe_3O_4, close to Fe_3O_4. Hence, it may be assumed that the oxide formed at the surface of the alloy 304L at the early beginning of its oxidation is composed of magnetite with traces of wüstite, undetectable by XRD.

Then, for greater oxidation times, XRD shows that chromia progressively vanished and converted into chromite. If the progressive disappearance of chromia is also observed in XPS analyzes, the formation of chromite is not seen at all, and neither the position of the iron peaks nor those of chromium exhibits any change. This proves that the solid-state reaction giving the chromite phase did not occur near the outer interface (oxide/gas) but inside the oxides layer.

Otherwise, it is worth reminding that the composition of the surface oxide shifts during the first hour of oxidation. Table 3 provides the Fe^{3+}/Fe^{2+} ratios determined on the basis of the peaks areas, according to the weight gain of the reaction. The satellites peaks were not considered for this calculation and the areas were estimated after that the Shirley-type background was subtracted. Even if the uncertainty on the measures is not known and probably rather high, a constant evolution appears on the values, going from 1.8 for $\Delta m/S \approx 0.02\,mg\,cm^{-2}$ (*i.e.* between $Fe_{1-x}O$ and Fe_3O_4, close to Fe_3O_4 as mentioned upper), to 2.5 for $\Delta m/S \approx 1\,mg\,cm^{-2}$ (*i.e.* between Fe_3O_4 and Fe_2O_3, always close to Fe_3O_4). So it appears that the composition of the outer surface of the oxide layer shifted from Fe_3O_4 containing traces of $Fe_{1-x}O$ at the early beginning to Fe_3O_4 containing traces of Fe_2O_3 after 1 h oxidation.

Table 3
Fe^{3+}/Fe^{2+} area ratio for different weight gains.

Weight gain ($mg\,cm^{-2}$)	Fe^{3+}/Fe^{2+} area ratio
0.02	1.8
0.09	2.3
0.3	2.4
1	2.5

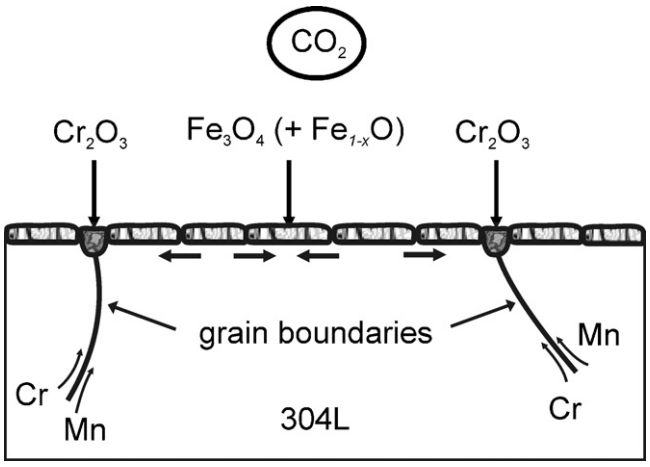

Fig. 5. Schematic cross section of 304L steel at the early beginning of the oxidation (near the surface).

4.2. Reaction mechanism

These results allow completing and slightly modifying the reaction mechanism that has been recently presented [1]. It is very complex and it has not to be presented again exhaustively here. Nevertheless, three points can be clarified now:

(i) At the early beginning chromia appears mainly at the grain boundaries [1], but, on the rest of the surface, the spinel phase is not composed of chromite but of magnetite Fe_3O_4 (with traces of wüstite $Fe_{1-x}O$). Fig. 5 schematises this step of the reaction, the arrows representing the intense flow of chromium at the grain boundaries, accompanied by manganese.
(ii) Afterwards, chromite forms inside the oxide layer, probably by solid–solid reaction;
(iii) For $\Delta m/S >$ around $0.3\,mg\,cm^{-2}$, when all the chromium of the surface grains has been oxidized, wüstite appears quantitatively (see XRD patterns) above the chromite phase, near the surface, because of an outward flow of ions Fe^{2+}. But on the

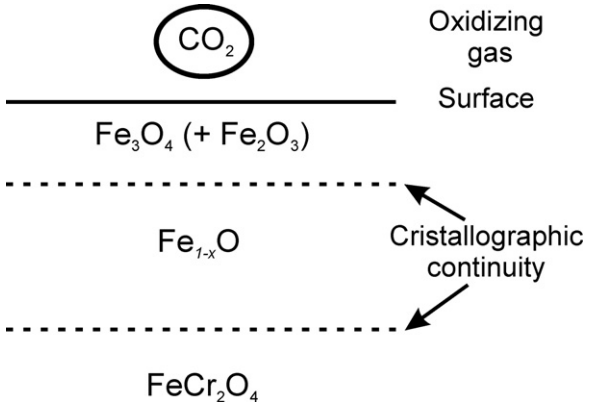

Fig. 6. Schematic cross section of the outer part of the oxide scale for samples partially oxidized ($0.3 < \Delta m/S < 1.15\,mg\,cm^{-2}$).

surface itself, probably on a weak thickness, it is always Fe_3O_4 that is in contact with CO_2 (with traces of hematite Fe_2O_3 for $\Delta m/S$ approaching 1 mg cm^{-2}). It is highly probable that a crystallographic continuity exists between the outer atomic plans of magnetite and the inner wüstite, and Fig. 6, which summarizes the situation of the surface zone, brings to the fore the slight transition between the successive phases present, when going inwards the oxides layer. This organization of the surface phases remains until the oxide scale split off from the substrate, for $\Delta m/S > 1.15$ mg cm^{-2} [1].

5. Conclusion

XPS analyzes modify significantly the model of oxidation of 304L steel in CO_2. Despite of the very few data on the oxides that may form in such experimental conditions, reliable conclusions could be drawn, which establish that the outer oxide formed is always magnetite. This phase coexists with chromia containing manganese located at the grain boundaries at the beginning of the reaction. It is also perhaps susceptible of slight variations of composition, with traces of wüstite (at the early beginning of the reaction) or hematite (before the split off of the oxide layer).

This point has some importance if the oxidation of the alloy is the first step for its thermal plasma coating. Actually, when a coating is processed by this way, the first splats deposed may keep the crystallographic structure of the underlying solid. It is the case for alumina deposits when the outer oxide layer is magnetite Fe_3O_4, as it was shown in the case of the junction between an alumina coating and a substrate of pre-oxidized alloy C40E [3]. In such conditions, the bonding between the deposit and the substrate is excellent, and the present results are promising for the good adherence of alumina plasma deposits on so pre-oxidized alloy 304L.

Moreover, during the oxidation of alloys, the external oxide layer is generally considered as composed of the most oxidizable metal of the alloys (here the chromium, forming chromia). The unexpected presence of magnetite, since the early beginning of the reaction under CO_2, opens interesting fields of research concerning the oxidation of other iron-based alloys.

References

[1] F. Goutier, S. Valette, A. Vardelle, P. Lefort, Corros. Sci. 52 (2010) 2403–2412.
[2] S. Valette, A. Denoirjean, D. Tétard, P. Lefort, J. Alloys Compd. 413 (1–2) (2006) 222–231.
[3] S. Valette, G. Trolliard, A. Denoirjean, P. Lefort, Solid State Ionics 178 (5–6) (2007) 429–437.
[4] S. Valette, A. Denoirjean, P. Lefort, Surf. Coat. Technol. 202 (2008) 2603–2611.
[5] P.A. Tempest, R.K. Wild, Oxid. Met. 23 (3–4) (1985) 207–235.
[6] V.E. Heinrich, P.A. Cox, The Surface Science of Metal Oxides, Cambridge University Press, Cambridge, 1994, p. 227.
[7] A.P. Grosvenor, B.A. Kobe, M.C. Biesinger, N.S. McIntyre, Surf. Interface Anal. 36 (2004) 1564–1574.
[8] R.P. Gupta, S.K. Sen, Phys. Rev. B: Solid State 12 (1) (1975) 15–19.
[9] L. Yin, I. Adler, T. Tsang, L.J. Matienzo, S.O. Grim, Chem. Phys. Lett. 24 (1) (1974) 81–84.
[10] M.G.C. Cox, B. McEnaney, V.D. Scott, Philos. Mag. 31 (2) (1975) 331–338.
[11] M.A.E. Jepson, R.L. Higginson, Corros. Sci. 51 (2009) 588–594.
[12] M.C. Biesinger, C. Brown, J.R. Mycroft, R.D. Davidson, N.S. McIntyre, Surf. Interface Anal. 36 (12) (2004) 1550–1563.